Determination of Effective Thermal Properties of Open Cell Ceramic Foam

Dr. Abdulhassan A. Karamallah
Machine and Equipment Engineering Department, University of Technology/ Baghdad.
Ali Mohammed Hussein
Machine and Equipment Engineering Department, University of Technology/ Baghdad.
Email: alimechanical_eng@yahoo.com

Received on: 7/8/2013 & Accepted on: 6/2/2014

ABSTRACT

This work presents an experimental investigation for effective thermal properties of open cell ceramic foam (80.13 Al_2O_3, 17.79 SiO_2, 1.57 MgO, and 0.51 Na_2O. % weight),which were measured using the Transient Plane Source (TPS) technique, and the parameters, which influenced them, and the influence of foam structure. Three types of pore per inch (ppi) were tested (10, 30 and 50). Three sensors were used, K5599 (of 60 mmdiameter), K4922 (of 30 mmdiameter) and K5501 (of 13 mmdiameter).The percentage difference between the highest and lowest results for each sensor and ppi are: for K5501 sensor were 34% in 10 ppi, 15% in 30 ppi and 18% in 50 ppi, for sensor K4922 were 19%, 11% and 13%, respectively, and for K5599 were 17%, 14% and 16%, respectively. The results show that the sensor K4922 is the more suitable sensor to test such material especially which has high ppi.

حساب الخصائص الحرارية الفعالة للرغوة السيراميكية مفتوحة الخلية

الخلاصة:

يقدم هذا البحث دراسة عملية للخصائص الحرارية الفعالة للرغوة السيراميكية مفتوحة الخلية بتركيب كيميائي حسب النسب الوزنية (80.13 Al_2O_3, 17.79 SiO_2, 1.57 MgO, and 0.51 Na_2O)والمقاسة بإستخدام تقنية Transient Plane Source (TPS). ايضا دراسة جميع العوامل المؤثرة في القياس بما فيها تأثير البناء الداخلي للرغوة السيراميكية. تم استخدام عدة انواع من الرغوة تختلف فيما بينها بحجم الخلية او عدد الخلايا خلال الإنج الواحد (ppi). أيضا تم استخدام ثلاث احجام من المستشعرات و هي K5599بقطر 60 mm, K4922بقطر 30 mm و K5501بقطر 13 mm. يبلغ مقدار الإختلاف بين أعلى وأوطئ قيمة كنسبة مئوية بالنسبة للمتحسسK5501 كما يلي 34% مع 10 ppi و 15% مع 30ppi و18% مع 50ppi ايضا للمتحسس الأوسط K4922 كما يلي 19% ،11% و 13% على التوالي، وبالنسبة للمتحسس الكبير 17% ، 14% و 16% على التوالي. النتائج اظهرت كفاءة المتحسس من نوع K4922كأفضل متحسس لقياس الرغوة السيراميكية خاصة مع الأنواع التي تكون ذات خلايا صغيرة او تمتلك عدد كبير من الخلايا للإنج الواحد.

https://doi.org/10.30684/etj.32.8A1
2412-0758/University of Technology-Iraq, Baghdad, Iraq

INTRODUCTION:

There is a plenty of application for open cell ceramic foam. For example, ceramics were used in the casting industry for filtration of molten metals. Since the 1960s, the filters made of ceramic materials were used in casting process, and the interest in these materials starts to increase. Millions of filters were made to remove inclusions which size down to the micron range. Although the foam structures were widely applied no established measuring method for determining the effective thermal conductivity of open cell ceramic foam exists. Many applications use the cellular ceramics or ceramic foams especially applications included high temperatures, like liquid metal filtration [1], gas filtration, heat exchanger, porous burners, and many other applications[2,3,4,5]. This wide range of ceramic foam applications attributed to its wide range of properties that come from both solid and fluid components. Properties like high permeability, low density, low specific heat and high thermal insulation, also cell size, morphology, and degree of interconnect are important factors that influence potential applications for those materials [2,3,6]. In general, the close cell foams are needed for purpose of insulation, while the open cell foams are used for fluid transport as filters or catalysts. This wide range of different properties needs a wide range processing routes to manufacture them. This led to a variety of production methods. The first and oldest one is Shwartzwalder method. It was based on replication of polymer foams by applying the ceramic slurry that is dried in place prior to the polymer template being burnt out and the ceramic sintered. Ceramic foams manufactured by this method are always open cell, have relative density between 5-30%, typical compression strength is in the range of for relative density up to 30%, reticulated foams, burning out the polymer leaves hollow and damage strut that can reduce the mechanical properties of the final foams significantly. Despite this, these foams are manufactured in large quantities and used extensively in filtering molten materials [7,8]. The second is the direct method relies on making bubbles inside the ceramic slurry by either mechanical agitation or in situ evolution of gases. This method probably yields to a widest range of cellular structures and properties, but they are generally less opening than the replicated foams and the compression strength reach 30MPa for relative density of 30% [8]. The third one is the burn-out fugitive pore relies on incorporation of sacrificial additive in the form of beads or related materials. Depending on the quantity added, it has been possible to produce micro-cellular ceramic foams, both from pre ceramic polymer precursors and conventional ceramic powder slurry, with cell size ranging from 1-100μm and possessing enhanced mechanical properties [8]. the foams can be predominantly open or close in nature. The open cell foam is porous material, define as two phase medium with a bulk matrix as a solid phase and pores containing the liquid phase. It is either a natural materials, like sand or industrial material, like foam. The most important property in porous medium is its porosity. It is defined as the fraction of void space in the material and given by [9] $\varepsilon = V_p/V_T$. Where, V_p is the pore volume and V_T is the total volume of the sample. The porosity comes from three types of spaces inside a cell (pore). The first type is the main hole of the cell. The second type is strut porosity, where the struts may contain holes inside them. The latter one is the material's porosity; all materials have micro-holes in their body. The overall porosity is a result of summation the above three kinds of porosity. There are many techniques to measure the porosity in literatures [10, 11, 12, 13, 14]. The heat transfer mechanisms in porous media are thermal radiation between solid elements,

thermal conduction in solids, thermal conduction in fluid, and thermal convection from solid to fluid. The effective thermal conductivity is measured as a result of these mechanisms. All mechanisms take place at the same time because of the very small area inside the porous media and randomly structure. This work does not include thermal convection because the pores are very small and there is no fluid flow, therefore, the rate of convection heat transfer is very small and can be neglected. Because of this, no direct way to calculate the effective thermal conductivity. The scientist derive many correlations for it, all of them depend the thermal conductivity of both solid and fluid parts. The difference between each other is in the assumption that was based on. **Russell [15]**proposed a correlation for high porosity foams. He analyzed the conduction through a solid matrix with cubic cells arranged in-line assuming a uniform cell-wall thickness and ignoring. When **Bhattacharya et. al.[16]**obtained a correlation for foam form a complex array of interconnected strut with an irregular lump of material intersection of two struts. They assumed in their model a two dimensional array of hexagonal cell, the lump was taken in account by considering a circular blob of the material at the intersection. **Boomsma and Poulikakos[17]**investigated analytically a geometrical effective thermal conductivity model of saturated porous metal foam, based on the idealized three-dimensional basic cell geometry of foam. The foam structure was represented with cylindrical ligaments which attach to cubic nodes at their centers. **Carson et. al. [18]** derived a model of effective thermal conductivity. They divided the porous media into internal porosity which has bubbles/pores suspended within a continuous condensed phase (e.g., sponges, foams, honeycombs), and external porosity which includes granular/particulate materials. When, **Park et. al. [19]** derived a new model of effective thermal conductivity of composite materials and included micro-balloons. **Petraschet. al. [20]**determined the effective thermal conductivity of reticulate porous ceramics based on the 3D digital representation of their pore-level geometry obtained by high-resolution multi-scale computer tomography. Also the scientist performed experiments using many methods to measure the thermal conductivity. **Suleiman et. al. [21]**used the transient plane source technique in a cryogenics temperature (88-280 K).They found that, the thermal conductivity value depends on the thermal history of the ceramic material. When, **Hsu and Howell [22]** used guarded hot plate in high temperatures (300-800 K).They found that the effect of natural convection within the porous plates with heating from below was found to be negligible. The measured conductivity decreased slightly as the pore size of the Partial Stable Zirconia (PSZ) increased. **Garcia et. al. [23]**and **Ali et. al. [24]** used the laser flash method the measure the thermal diffusivity, and by available value of density and heat capacity, they could calculate the thermal conductivity. **Garcia et. al. [23]**studied two type of foam with 10% difference in porosity. They found that, the difference in results did not just by the effect of porosity, but the difference in composition may be important too. **Ali et. al. [24]**investigated the highly porous zirconia ceramic. The porosity was varied from 45 to 75% by adjusting the thermal treatment between$750$and $1100\ °C$. Thermal diffusivity measurements were made with the laser flash technique in order to determine the thermal conductivity at room temperature. **Lo et. al. [25]** performed the experiments using the transient line source in high temperature. The result showed that, for the ceramic foam with 93.9% and 94.5%porosities have thermal conductivity values of$0.085\ W/mK$and$0.055\ W/mK$, respectively. At $800\ °C$, the thermal conductivity values of Al_2O_3 with the porosity of 93.9% and 94.5% are $0.21\ W/mK$and $0.14\ W/mK$, respectively, which are several times greater than

those at room temperature. High porosity, large cell size, and smaller grain size are responsible for the low conductivity.

The present work studies the effect of foam structure on the effective thermal conductivity in room temperature. Also, studies the effect of sensor size of the Transient Plane Source method on it.

Theory of the Hot Disk analyzer:

The TPS system is one of the transient methods which is used to measure thermal transport properties. To use these methods efficiently, the specimen needs to be in thermal equilibrium with the environment or the surrounding. Then, a short heating pulse is given to the specimen. During the time of measurement, the change in temperature is monitored and a curve plotted as shown (Fig.1). By correlating the experimental temperature records with the theoretical formulas (Fig.2), the thermal diffusivity is determined. The TPS method considers three dimensions of heat diffusion inside the specimen, and it is regarded as an in finite medium [31].

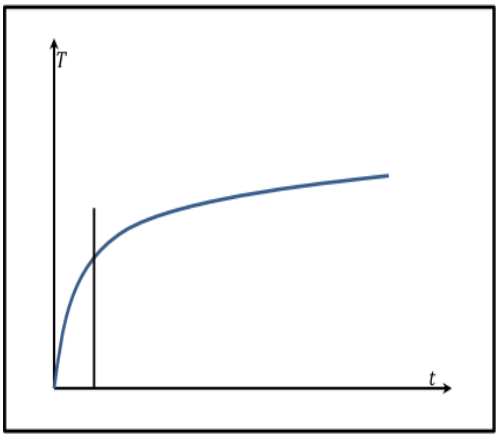

Figure.(1)Measuring data by TPS technique

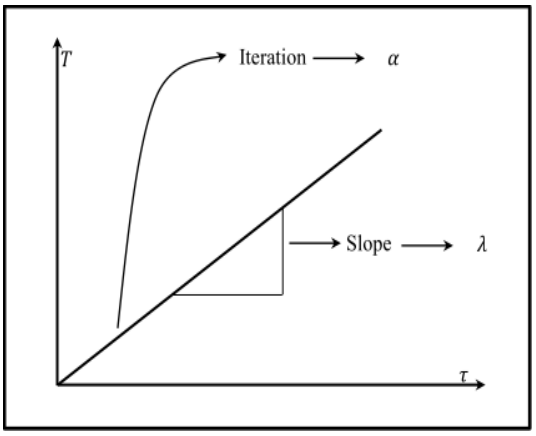

Figure.(2)Resulting line after curve fitting

The thermal diffusivity is obtained through the curve fitting process. The curve fitting processis achieved by assume a value for the thermal diffusivity and use it to find the dimensionless by this expression:

$$\tau = \frac{\sqrt{\alpha t}}{a} \quad \text{... (1)}$$

Where, τ is the dimensionless time. $t$is duration of the experiment. $a$is the sensor's diameter. After that, the program substitutes the value of the dimensionless time in the temperature difference equation:

$$\overline{\Delta T(\tau)} = \frac{P_\circ}{a\,\lambda_{eff}\pi^{3/2}} D(\tau) \quad \text{… (2)}$$

Where, $D(\tau) = \frac{1}{m^2(m+1)^2}\int_0^\tau \frac{d\sigma}{\sigma}\sum_{k=1}^{m}\frac{ka}{m}\cdot\sum_{l=1}^{m} lae^{\left(-\left(\left(\frac{k}{m}\right)^2+\left(\frac{l}{m}\right)^2\right)/4\sigma^2\right)}.I_o\left(\frac{kl}{2\sigma^2m^2}\right)$

$P_\circ$is the power released from the sensor. $\lambda$is the thermal conductivity. $m$is the number of the rings of the sensor. $k, l$are counters. $\sigma$is a transformation function. The program repeat this process until equation (2) convert to an equation of a straight line. Then,

the value of the thermal diffusivity that makes it for a straight line is the value that we need it. Then, by calculating the slope of the straight line and equalized it with the coefficient in equation (2), the program finds the thermal conductivity.

As mentioned above, the Hot Disk analyzer is a fully electric device, therefore; it deals with electrical function like resistance. The device measures the resistance and converts it to a temperature difference using the following equation:

$$R(t) = R_0 \left[1 + TCR\, \overline{\Delta T(\tau)}\right] \quad \ldots (3)$$

Where, $R_0$is the resistance of the TPS element before the transient recording has been initiated.$TCR$is the temperature coefficient resistivity. $\overline{\Delta T(\tau)}$is the properly calculated mean value of time dependent temperature increase of the TPS element.The program calculates the heat capacity per unit volume by using:

$$\rho C = \lambda/\alpha \quad \ldots (4)$$

Experimental apparatus:

The Hot Disk analyzer is based on supplying constant power to samples in isothermal condition by the sensor during limited experiment time. The temperature increase is recorded by the sensor also act as resistance thermometer. The dynamic features of the temperature increase, reflected in resistance increases of the sensor, are precisely recorded and analyzed, so that both the thermal conductivity and thermal diffusivity can be determined from one single transient recording. [26, 27]

Because of fully electrical construction of the Hot Disk device, there is no interesting thing inside it except the resistance measuring circuit or in other word Wheatstone bridge circuit. As illustrate in (Fig.3), the circuit contains many types of resistance.$R_p$is the resistance of wires.$R_s$is a standard resistance with a current rating that is much higher than $I_\circ$, which is the initial heating current through the arm of the bridge containing the TPS-element.$R_1$is another known resistance in the side of fix resistances of Wheatstone bridge. On the opposite side of Wheatstone bridge there areR_2 which is the variable resistance and R is the sensor resistance.

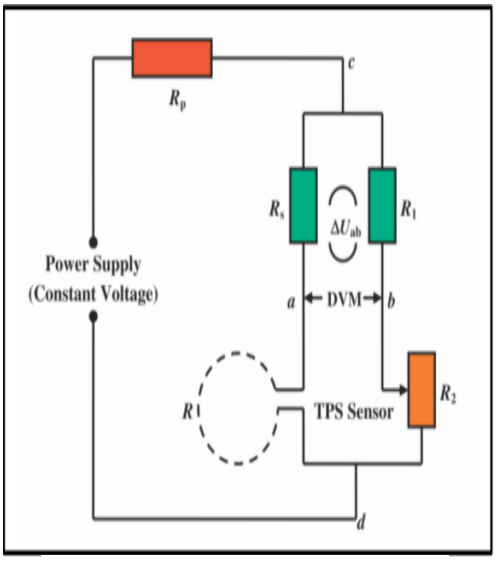

Figure.(3) Measuring circuit of sensor's bridge[28,29,30]

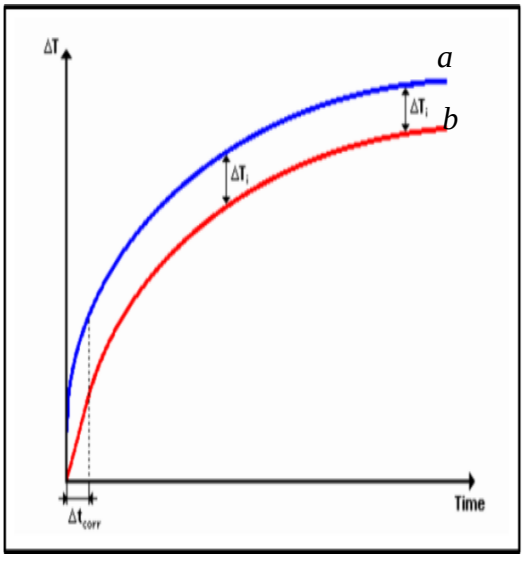

Figure (4) Sensor and sample temperature increase[26, 29] 1.Red line for sensor 2. Blue line for specimen

The Hot Disk device needs to measure the resistance of the sensor each time performs experiment. This comes from many types and sizes of sensors. Also, in one sensor the resistance changes through heating. This measured resistance is transformed to a temperature difference. The sensor always measures the temperature on its surface, but the temperature distribution appeared to observer is for the specimen. This is because there is a temperature difference between the sensor and specimen due to the contact. This temperature difference is illustrated in Fig.4. Where, the line *a*is for the sensor and line *b* is for specimen. The reader can see that after a while the temperature difference will be constant. This time can be estimated approximately by:

$$\Delta t = \frac{\delta^2}{\alpha} \quad \ldots (5)$$

Where, t is the time, δ is the thickness of sensor.$\alpha$is thermal diffusivity.

The Hot Disk sensor is contained an electrically conduction material shaped in double spiral of Nickel which is placed out of thin sheet. Nickel was chosen because of its high and well-known temperature coefficient of resistivity. It is covered on both sides with thin foil of electrical insulation. The TPS system can measure from cryogenics about $30\ K$ to $1000\ K$ and might be extended to $1800\ K$ when using special types sensors. For this reason, there are two types of insulation. The first is Kapton, with foil thickness of$12.5\ \mu m$ or$25\ \mu m$. This makes the total thickness of the sensor between$60$and$80\ \mu m$. This insulation covers from cryogenics to $500\ K$. The second one is Mica for high temperatures, with foil thickness $0.1\ mm$, this incereases the total thickness of the sensor to$0.25\ mm$. [26,28,29,30]. It is not recommended to use the sensor with mica insulation in experiment performed at temperature less than $500\ K$ due to the low sensivity and accuracy caused by thicker insulation [26]. Three sizes of Kapton sensors were used in work (K5599, K4922, K5501). Figure.5illustrates all the types that are in this work.

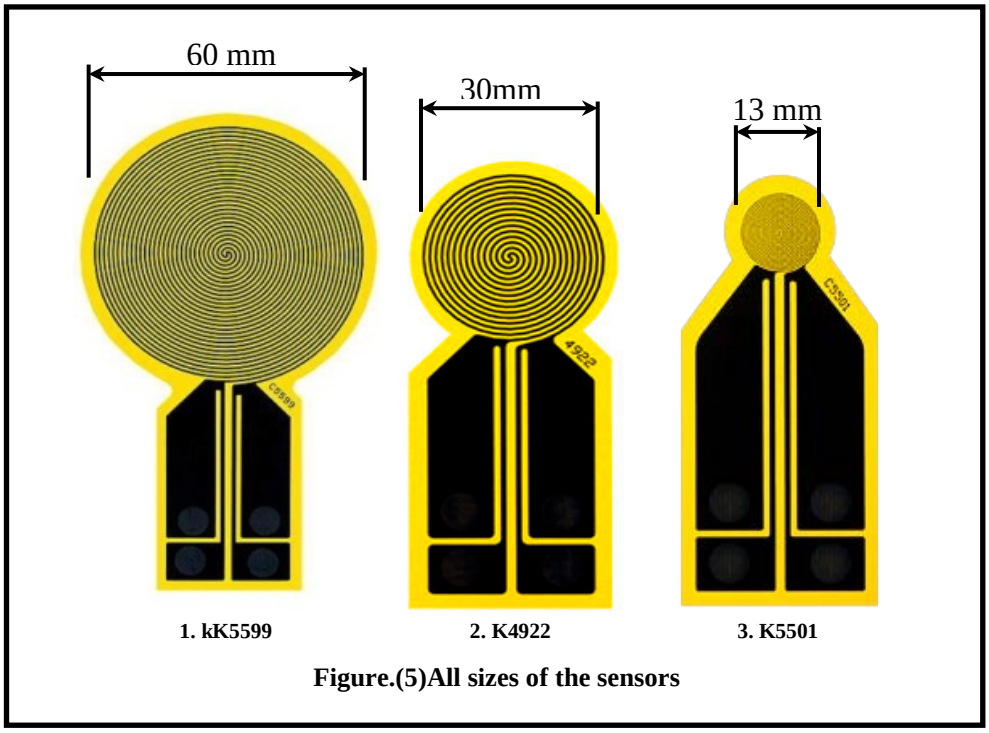

Figure.(5)All sizes of the sensors

Experimental procedure:

A. Sample preparation:

The open cell ceramic foam sheets are manufactured by Drache Umweltechnik GmbH Company. The materials components which samples were made of were for 10 ppi samples (69.6 Al_2O_3, 26.22 SiO_2, 3.45 MgO, and 0.73 Na_2O. %Moll). For 30 ppi is (70.61 Al_2O_3, 26.28 SiO_2, 2.75 MgO, and 0.73 Na_2O. % Moll).Also for 50 ppi is (72 Al_2O_3, 25.63 SiO_2, 1.97 MgO, and 0.4 Na_2O. % Moll). The specimens were cut in dimensions 160x160x50 mm. These dimensions were taken, because the specimen width or diameter must be at least two times the sensor's diameter, also the thickness should not be less than the sensor's diameter. The specimens were cut with electric saw designed for cutting foams. After cutting, one of specimen's faces should be grinded in order not to be scratchy or destroy the sensor and also to increase the contact area. The grinding process was performed by three levels according to the roughness of grinding sheet used. The roughness of grinding sheets is $54\ \mu m, 10\ \mu m\ and\ 3\ \mu m$. The small one is for finishing the smooth surface of the specimens. By the process above, were made eight specimens were made in each kind of these ppi (10, 30 and 50).

B. Procedure of experiments:

The experiment itself is easy to perform, but the whole measurement takes long time, because the sensor and the specimen need time to return to their equilibrium state. The time between experiments differs according to the set time of experiment. There are three parameters should be in their range to accept the measurement and its results. Also, the user should check the stability of the measurement by continuing change the number of data point in step of calculation. If it is stable, it must not change in the amounts of results or a very small variation, it would be acceptable. The parameters that must stay in their ranges are:

1. <u>Penetration depth (probing depth)</u>: is the longest straight distance that the heating power transfers from the sensor to the specimens in any direction. It is given by [32,33]:

$$\Delta p = 2\sqrt{\alpha t_{max}} \ldots \quad \ldots (6)$$

Where, t_{max} is the time installed for the measurement. This relation shows that to get an accurate thermal conductivity and diffusivity in easy way, the specimens should be large [26]. The limit of the penetration depth is the shortest straight distance from the edge of the sensor to the nearest border of the specimen. It is very important to know the limits of penetration depth. If the penetration depth is beyond its limits, this means that the sensor affect with material outside the border of the specimen. Because outside the specimen is air, may be someone ask that this work deals with foam and the foam have high amount of air included. The answer is anything inside the boundaries is a part of the specimen.

2. <u>The dimensionless time</u>: to use many ranges of time in efficient way. The program converts the time to a dimensionless time. The relation used for this purpose is Eq. (1). In the derivative, the integral boundaries are from 0 to τ. This means that the dimensionless is not an exact number, but it is a range found to be between (0.33 – 1) [26], and this range is the limit of dimensionless time.

3. <u>Temperature increase</u>: the increase in the temperature here is only between the sensor and parts of specimen near the sensor. When the temperature increases as a function of the dimensionless time, it has also a range. According to dimensionless time, the temperature increase's range is between $(1-3\,K)$. The average increase in the temperature is governed by Eq. (2).

Results and Discussion

This section discusses and compares the measurements that were performed with three types of sensors (K5501, K4922 and K5599). There are three parameters that control each thermal property according to Eq. (1), (2), and (6). So, it is impossible to say, for example, that one parameter temperature difference influences on the thermal conductivity without taking into account the effect of sensor size and the heat flux. Rearranging Eq. (3) to include the heat flux by multiplying it with (a/a) and assuming that the area of heating coil of the sensor is πa^2:

$$\lambda_{eff} = \frac{\dot{q}a}{\overline{\Delta T(\tau)}\pi^{1/2}} D(\tau) \qquad \dots (7)$$

Where, $\dot{q}$ is the heat flux, and the same think for thermal diffusivity, it is controlled by dimensionless time, sensor's size and the duration of the test (Eq. (1)) or by maximum time set for test and the probing depth, Eq.(6). Heat capacity is always determined by both thermal conductivity and diffusivity. By taking a look at graphs that belong to 10 ppi, Figs.(6, 7) and (8); it is easy to say that the sensor K5501 is not good to measure this material. This proves that with a material having a void fraction, it is suitable to use a large sensor with 60 mm in diameter [26]. But, it is very difficult to say the measurements are good and stable even with this hint from the manual of the device [26]. The void fraction or the porosity is almost the same for all specimens in all ppi. So, the porosity has no influence but the pore size or the pore per inch and the matrix of the foam have effects. It is well known that the heat transfer mechanisms in this work are radiation between solid elements, conduction in solid and conduction in air. The 10 ppi has a big pore size and relatively uncomplicated matrix as compared with 30 and 50 ppi which are making the polished parts big and little. This means that, for the small sensor K5501, it is difficult to conduct the heat through the air, so one of the mechanism stops, and this gives unstable measurements. Also, for the big sensor K5599, the power is relatively small compared with sensor's size. But, the big size means high contact area so the measuring is stable more than the case with K5501. For sensor K4922 that has the medium size with suitable power make, the measurements are stable more than others. For the graph of thermal diffusivity, Fig.(7), one can see that the ranges of thermal diffusivity for all sensors are too high. This is logical with the matrix and the pore size of 10 ppi specimens. Heat diffused fast, especially for K5501 through these specimens by radiation due to big amount of air. Table.(1) contains the average values of the measurements' results for 10 ppi with all sensors. One can see also that the average values of the thermal conductivity are quite the same, but this does not mean that the results are good.

Table.(1)An average values of measuring 10 ppi samples

Sensors	Kapton 5501	Kapton 4922	Kapton 5599
Power (W)	0.1	0.5	0.5
Max. time (s)	20	160	360
Heat flux (W/m^2)	753.778	757.363	182.976
λ(W/mK)	0.507	0.488	0.496
α(mm^2/s)	1.579	0.906	1.205
c_p(MJ/mm^{3}K)	0.333	0.545	0.42
Δp (mm)	11.48	24.06	38.86
τ	0.813	0.68	0.437
ΔT (K)	1.406	2.919	1.513
Sensor's area (m^2)	132.665	660.185	2732.585
Sensor's size (mm)	13	29	59

For 30ppi graphs Figs.(9, 10) and (11), one can see that the measurements are more stable than 10 ppi. This is because the 30 ppi specimens approach from the dense materials by their matrix shape. In Fig.9, one can see also that K5501 is still not good for measuring as compared with others (K4922 and K5599). This returns to the same reason that for porous material, it is good to use big sensors [66]. In Fig.(10), one can see that the ranges of thermal diffusivity for all sensors are too high but not higher than that in 10 ppi. This also returns to the same reason of heat diffusion inside the specimen by radiation. Also, because the matrix for 30 ppi is more complicated, the thermal diffusivity is not too high as compared with 10 ppi. This high variation in thermal diffusivity affects the heat capacity, Fig.11. In table.(2), one finds an average value of measurements' results of 30 ppi. For K5501, the thermal conductivity is higher than others, while the heat flux is not too high. This is also returning to other parameters, like temperature difference and sensor size. Although a small value of sensor size, but the small value of temperature difference raises the amount of thermal conductivity. Also, the indirect effect of the dimensionless time on the dimensionless function makes it high. For K4922 and K5599, the temperature difference is quite the same, but the heat flux has a big difference. So, the effect of sensor size put the thermal conductivity values near from each other. For the thermal diffusivity, one can say it depends on the dimensionless time and sensor size according to Eq.(2) or on the probing depth according to Eq.(6). In both cases, it is clear why K5599 has high thermal conductivity.

Table (2) An average values of measuring 30 ppi samples

Sensors	Kapton 5501	Kapton 4922	Kapton 5599
Power (W)	0.1	0.8	1
Max. time (s)	40	160	360
Heat flux (W/m^2)	753.778	1211.782	365.954
λ(W/mK)	0.504	0.442	0.422
α(mm^2/s)	0.852	0.836	1.083
c_p(MJ/mm^{3}K)	0.6	0.531	0.392
Δp (mm)	11.668	23.125	40.286
τ	0.83	0.628	0.47
ΔT (K)	1.371	2.98	2.906
Sensor's area (m^2)	132.665	660.185	2732.585
Sensor's size (mm)	13	29	59

For 50 ppi, Figs.12, 13 and 14, the matrix approaches more from the dense material. Therefore one sees that the range of measurements' results is small, especially for both thermal conductivity and diffusivity. For the thermal conductivity, Fg.12, the measurements of K5501 go far, because these still have high void fraction and need a big sensor for measuring [66]. The thermal diffusivity, Fig.13 for K5501, has wide range with low values. This means that the complicated matrix of this type of filter foam does not allow heat to diffuse deeply inside the specimens, especially with low power released from the sensor. When, K5599 still has high thermal diffusivity due to its size and the high power released from it. For heat capacity, Fig.14, it is logical when with low thermal diffusivity there is high heat capacity and vice versa. This is because low diffusivity means, a big amount of the power stores inside the material, and this is the definition of the heat capacity. If one takes a look on the average values of the measurements' results, Table.3, he finds it is same behavior and effect of 30 ppi but with other numbers. For K5501, the temperature difference is lower than one; this makes the thermal conductivity jump to higher value.

Table (3)An average values of measuring 50 ppi samples

Sensors	Kapton 5501	Kapton 4922	Kapton 5599
Power (W)	0.05	0.75	1.5
Max. time (s)	40	160	360
Heat flux (W/m^2)	376.889	1136.045	548.9308
λ(W/mK)	0.53597	0.420821	0.3900964
α(mm^2/s)	0.69336	0.732442	1.03295
c_p(MJ/mm^{3}K)	0.777639	0.574942857	0.380542857
Δp (mm)	10.088	21.643	36.307
τ	0.6289	0.5497	0.3794
ΔT (K)	0.640	2.924	2.774
Sensor's area (m^2)	132.665	660.185	2732.585
Sensor's size (mm)	13	29	59

CONCLUSION:

This work has reached to the following conclusions:

1. In the measurement of different sensors and different ppi, the small sensor K5501 shows a stable mean value in all ppi types despite of the big deviation in the measurements.
2. The bigger sensors (K4922, K5599) show a drop in mean values with an increase in the ppi despite that the deviation in their measurements is too small compared with K5501.

Nomenclatures:

English symbols	
a	Biggest radius of the sensor (m)
c	Heat capacity (J/kgK)
$D(\tau)$	Dimensionless function $(-)$
$I_\circ$	Bessel function $(-)$
m	Number of ring of sensor $(-)$
$P_\circ$	Power release from sensor (W)
$\dot{q}$	Heat flux (W/m^2)
R	Electrical resistance (Ω)
R_0	Initial resistance (Ω)
T	Temperature (K)
TCR	temperature coefficient of resistivity $(1/K)$
t	Time (s)
V_p	Pore volume (m^3)
V_T	Total volume (m^3)

Greek symbols	
α	Thermal diffusivity (mm^2/s)
Δp	Probing depth (mm)
δ	Sensor thickness (m)
ε	Porosity $(-)$
λ_{eff}	Effective thermal conductivity (W/mK)
ρ	Density kg/m^3
σ	Transfer function $(-)$
τ	Dimensionless time $(-)$

REFERENCES:

[1] S. Ray, B. Milligan, N. Keegan,"Measurement of filtration performance, filtration theory and practical applications of ceramic foam filters",Aluminium Cast House Technology 2005.

[2] M. R. Nangrejo, X. bao, M. J. Edirisinghe, "The structure of ceramic foams produced using polymeric precursors", JOURNAL OF MATERIALS SCIENCE LETTERS19 (2000) 787–789.

[3] P. Colombo, M. Griffoni, M. Modesti, ”Ceramic Foams from a Preceramic Polymer and Polyurethanes: Preparation and Morphological Investigations”, Journal of Sol-Gel Science and Technology 13, 195–199 (1998).
[4] J. Vicente, F. Topin, J. Daurelle, ”Open Celled Material Structural Properties Measurement: From Morphology To Transport Properties”, Materials Transactions, 47, (2006) 2195-2202.
[5]M. J. Matos, S. Dias and F. A. Costa Oliveira, ”Macrostructural changes of polymer replicated open cell cordierite based foams upon sintering”, Advances in Applied Ceramics 2007.
[6] S.N. Jayasinghe and M.J. Edirisnghe, ”A Novel Method of Forming Open Cell Ceramic Foam”, Journal of Porous Materials 9: 265–273, 2002.
[7] J. Adler, G. Standke, ”Offenzellige Schaumkeramik, Teil 1” Keramische Zeitschrift 55 (2003).
[8] P. Colombo, ”Conventional and novel processing methods for cellular ceramics”, The Royal Society 2005.
[9] M. Kaviany, ”principle of heat transfer in porous media”, ISBN: 0-387-94550-4, 1995.
[10] T. W. Engler, ”Fluid Flow in Porous Media”, New Mexico Tech. 2010.
[11]N. Ezekwe, ”Petroleum Reservoir Engineering Practice”, ISBN-10: 0-13-715283-3/0-13-248521-4, September 14, 2010.
[12] J. Dorsch,”Determination of Effective Porosity of Mud rocks – A Feasibility Study”, Environmental Sciences Division, Oak Ridge National Laboratory, Oak Ridge, TN 37831-6352, 1995.
[13] Paul W.J. Glover,”Formation Evaluation MSc Course Notes”, University of Aberdeen UK. 2001.
[14] L. Palacio, P. Prädanos, J.I. Calvo, A. Hernández,”Porosity measurements by a gas penetration method and other techniques applied to membrane characterization”, Thin Solid Films 348 (1999) 22-29.
[15] Russell, "Principles of heat flow in porous insulators", Journal of American Ceramic Society (1935) 1–5.
[16] A. Bhattacharya, V. V. Clamidi, R.L. Mahajan, "thermophysical properties of high porosity metal foam", International journal of heat and mass transfer 45 (2000) 1017-1031.
[17] K. Boomsma, D. Poulikakos, "On the effective thermal conductivity of a three-dimensionally structured fluid-saturated metal foam", International Journal of Heat and Mass Transfer 44 (2001) 827-836.
[18] J. K. Carson, S. J. Lovatt, D. J. Tanner, A. C. Cleland, "Thermal conductivity bounds for isotropic, porous materials", International Journal of Heat and Mass Transfer 48 (2005) 2150–2158.
[19] Y. Park, J. Kim, J. Lee, "Prediction of Thermal Conductivity of Composites with Spherical Microballoons", Materials Transactions, 49 (2008) 2781-2785.
[20] J. Petrasch, B. Schrader, P. Wyss, A. Steinfeld"Tomography-Based Determination of the Effective Thermal Conductivity of Fluid-Saturated Reticulate Porous Ceramics", Journal of Heat Transfer, 130 (2008).
[21]B. M. Suleiman, I. Haq, E. Karawackit, S. E. Gustafssont. "Thermal conductivity of the ceramic Cecorite 130P between 88 and 288 K measured using the transient plane source technique", Journal of Physics 25 (1992) 813-817.

[22] P. Hsu and J. Howell."Measurements of thermal conductivity and optical properties of porous partially stabilized zerconia", Experimental Heat Transfer, 5 (1992) 293-313.
[23] E. Garcia, M. I. Osendi, and P. Miranzo, "Thermal diffusivity of porous cordierite ceramic burners", Journal of applied physics 92, 2346 (2002).
[24] B. Nait-Ali, K. Haberko, H. Vesteghem, J. Absi, D.S. Smith "Thermal conductivity of highly porous zirconia", Journal of the European Ceramic Society 26 (2006) 3567–3574.
[25] Y.W. Lo, W.C.J. Wei, C.H. Hsueh, "Low thermal conductivity of porous Al2O3 foams for SOFC insulation", Materials Chemistry and Physics 129 (2011) 326– 330.
[26] "Instruction Manual Hot Disk 6.1",2011, Hot Disk®,Ver.0.1.
[27] M. Gustavsson, E.Karawacki, S. E. Gustafsson."Thermal conductivity, thermal diffusivity and specific heat of thin samples from transient measurements with hot disk sensor", Rev. Sci. Instrum.65 (12), 1994.
[28] Gustafsson, "Transient plane source techniques for thermal conductivity and thermal diffusivity measurements of solid materials", Review Scietific Instrument 62 (3), 1991.
[29] A. Sharma, N. Mehta. "Analysis of composition dependence of some thermal transport properties in glassy alloys using transient plane source measurements", Measurement 46 (2013) 514–520.
[30] R. Mangal, N.S. Saxena, M.S. Sreekala, S. Thomas, K. Singh."Thermal properties of pineapple leaf fiber reinforced composites", Materials Science and Engineering A339 (2003) 281 285.
[31] L. Huang and L. Liu."Simultaneous determination of thermal conductivity and thermal diffusivity of food and agricultural materials using a transient plane-source method", Journal of Food Engineering 95 (2009) 179–185.
[32] O Almanza, M. Rodrıguez-Perez, JA de Saja. "Measurement of the thermal diffusivity and specific heat capacity of polyethylene foams using the transient plane source technique",PolymInt 53:2038–2044 (2004).
[33] Y. He, "Rapid thermal conductivity measurement with a hot disk sensor", ThermochimicaActa, 2005,122-129.

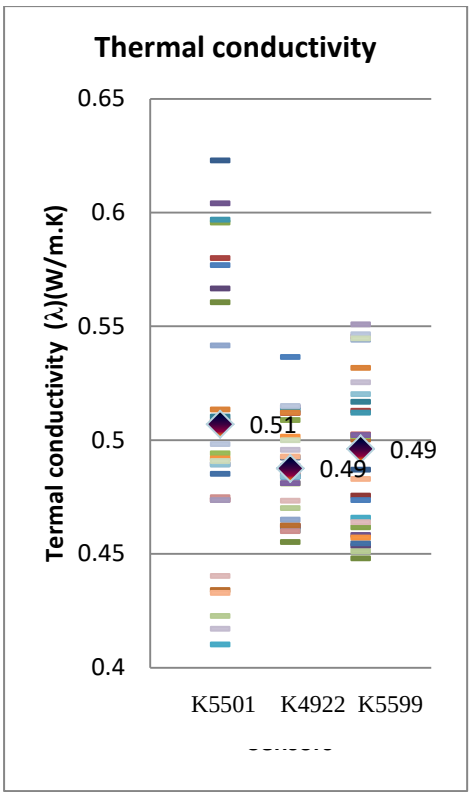

Figure.(6) Thermal conductivity vs sensors 10ppi

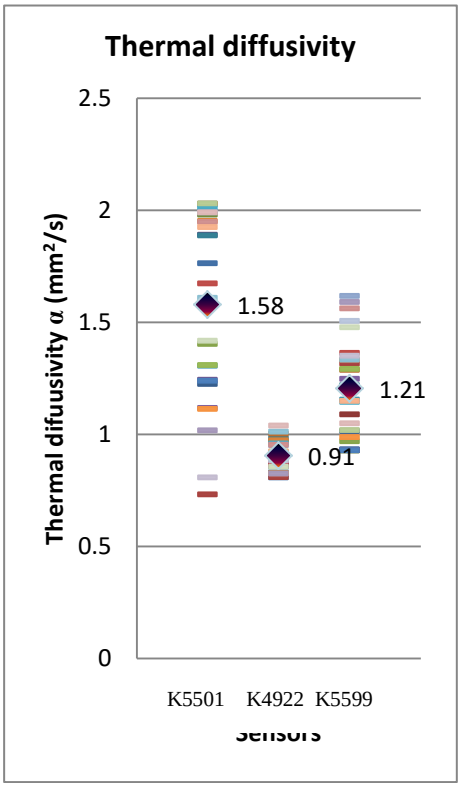

Figure.(7) Thermal diffusivity vs sensors10 ppi

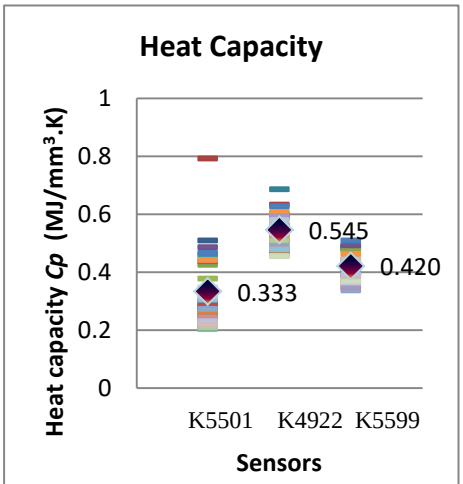

Figure.(8)Heat capacity vs sensors 10 ppi

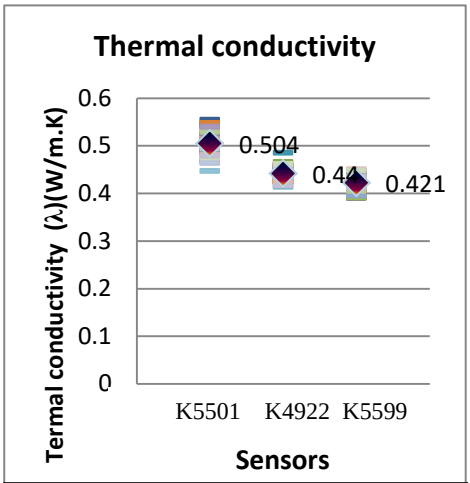

Figure.(9) Thermal conductivity vs sensors 30 ppi

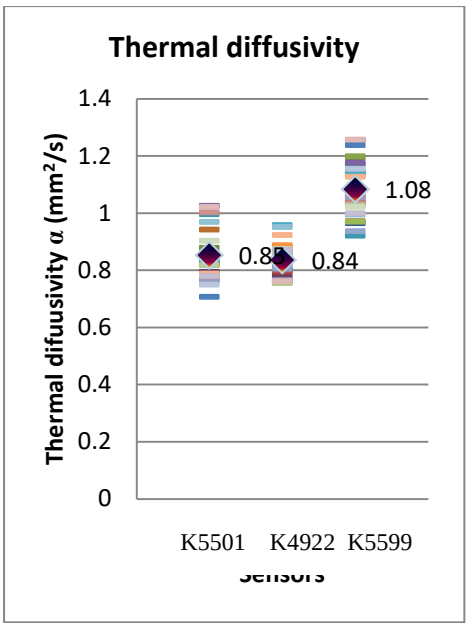

Figure.(10) Thermal diffusivity vs sensors30 ppi

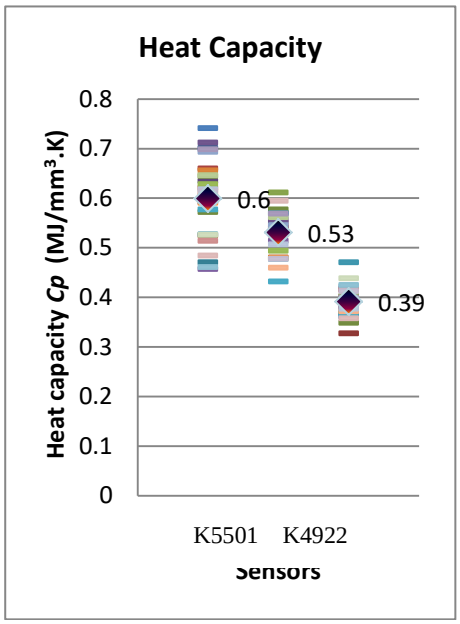

Figure.(11)Heat capacity vs sensors 30 ppi

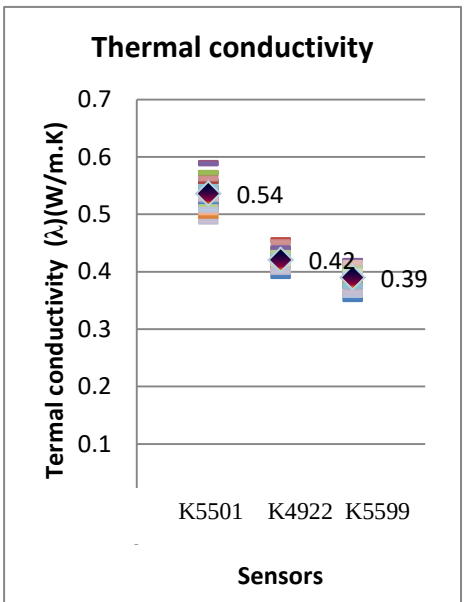

Figure.(12)Thermal conductivityvs sensors50 ppi

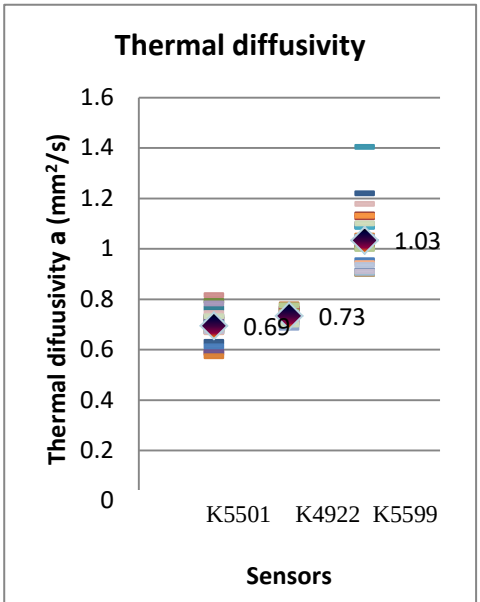

Figure.(13)Thermal diffusivity vs sensors50 ppi

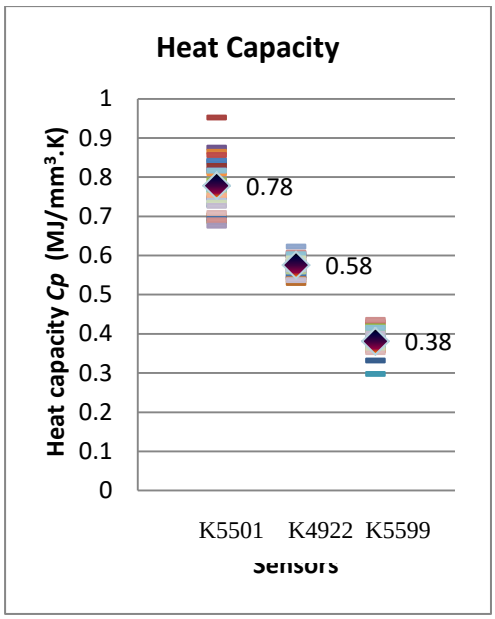

Figure.(14)Heat capacity vs sensors 50 ppi